



# Numerical simulation of the impurity photovoltaic effect in silicon solar cells doped with thallium

Baoxing Zhao, Jicheng Zhou\*, Yongmin Chen

School of Energy Science and Engineering, Central South University, Changsha 410083, China

## ARTICLE INFO

### Article history:

Received 5 January 2010

Received in revised form

4 June 2010

Accepted 4 June 2010

### Keywords:

Silicon solar cells

Impurity photovoltaic effect

SCAPS

Light trapping

## ABSTRACT

Many attempts have been made to increase the efficiency of solar cells by introducing a deep impurity level in the semiconductor band gap. Since Tl may be the most suitable impurity for crystalline Si solar cells, the impurity photovoltaic (IPV) effect in silicon solar cell doped with thallium as impurity was investigated by the numerical solar cell simulator SCAPS. Results show that the IPV effect of thallium extends the spectral sensitivity in the sub-band gap range from 1000 to about 1400 nm. When the Tl concentration ( $N_t$ ) is lower than the base doping density ( $N_D$ ), the short-circuit current density and efficiency increase with increasing  $N_t$ . But they decrease rapidly as the impurity density exceeds the shallow base doping density ( $N_t > N_D$ ). The optimum Tl concentration is about equal to the base doping density. For the Si solar cells with high internal reflection coefficients, the IPV effect becomes appreciable ( $\Delta J_{sc} \approx 9 \text{ mA/cm}^2$  and  $\Delta \eta \approx 2\%$ ).

Crown Copyright © 2010 Published by Elsevier B.V. All rights reserved.

## 1. Introduction

Silicon solar cells still represent about 80% of the production of semiconductor solar cells [1]. Different approaches have been suggested to further increase the conversion efficiency of these cells. The most important power-loss mechanism in the single band gap cells is the inability to absorb photons whose energy is less than the band gap [2]. The impurity photovoltaic (IPV) effect can effectively utilize this lost energy in principle. The approach is to introduce one or more impurity bands (IB) within the band gap of host semiconductor. These IB can help the solar cell to absorb sub-band gap photons, thereby increasing the short-circuit current ( $J_{sc}$ ) [3,4].

Schmeits and Mani have demonstrated numerically that the IPV effect could moderately improve the performance of crystalline Si cells [1]. Since then, a great deal of work has been done in the field of numerically simulated IPV effect, including IPV effect in GaAs solar cells [5,6], Si solar cell [4,7], and so on. Several approaches have been proposed to put the IPV concept into practice [8]. In, Zn and thallium (Tl) are typical deep level impurity in Si, and the IPV effects of the former two elements have been numerically demonstrated [7,9]. Besides, the optimum position of the deep level is theoretically at one-third of the band gap energy. However, Verschraegen found that the efficiency is maximal when the impurity is at 0.20–0.25 eV for the crystalline Si cells [10]. Therefore, Tl may be the most suitable impurity for

crystalline Si solar cells. Whereas the IPV effect of Tl impurity on silicon solar cells output performance has not been studied. In this work, we present a numerical study of the IPV effect in Tl-doped crystalline silicon solar cells with SCAPS [11].

## 2. Theory of impurity photovoltaic effect

In the Shockley–Read–Hall (SRH) recombination model, electron and hole transition through the impurity is governed by capture, thermal and optical emission of carriers. As illustrated in Fig. 1, the IB allows the absorption of sub-band gap photons: the absorption of photon  $h\nu_1$  pumps an electron from the valence band (VB) to the IB, while the absorption of photon  $h\nu_2$  causes an electronic transition from the IB to the conduction band (CB). The net recombination rate  $U$  via the impurity is given by [2,5]

$$U = \frac{np - (n_1 + \tau_{n0}g_{nt})(p_1 + \tau_{p0}g_{pt})}{\tau_{n0}(p + \tau_{p0}g_{pt}) + \tau_{p0}(n + n_1 + \tau_{n0}g_{nt})}, \quad (1)$$

$$\tau_{n0} = \frac{1}{c_n N_t} \quad \text{and} \quad \tau_{p0} = \frac{1}{c_p N_t}, \quad (2)$$

$$n_1 = N_C e^{-(E_C - E_t)/kT}, \quad p_1 = N_V e^{-(E_t - E_V)/kT}, \quad (3)$$

$$g_{nt} = N_t \int_{\lambda_{nmin}}^{\lambda_{nmax}} \sigma_n^{opt}(x, \lambda) \phi_{ph}(x, \lambda) d\lambda, \quad (4)$$

$$g_{pt} = N_t \int_{\lambda_{pmin}}^{\lambda_{pmax}} \sigma_p^{opt}(x, \lambda) \phi_{ph}(x, \lambda) d\lambda, \quad (5)$$

\* Corresponding author. Tel.: +86 13873193957.

E-mail address: [jicheng@mail.csu.edu.cn](mailto:jicheng@mail.csu.edu.cn) (J. Zhou).

where  $n_1$  and  $p_1$  are the electron and hole concentrations,  $\sigma_n^{opt}$  and  $\sigma_p^{opt}$  are the electron and hole photoemission cross-sections of the impurity.  $N_t$  is the density of the defect. Terms in  $g_{nt}$  and  $g_{pt}$  describe the IPV effect.

In a Lambertian cell, the photon flux  $\phi_{ph}(x, \lambda)$  at a depth  $x$  for photon wavelength  $\lambda$  is given by the following equation:

$$\phi_{ph}(x, \lambda) = \phi_{ext}(\lambda) \frac{1 + R_b e^{-2\alpha_{tot}(\lambda)(L-x)}}{1 - R_f R_b e^{-2\alpha_{tot}(\lambda)L}} e^{-\alpha_{tot}(\lambda)x}, \quad (6)$$

where  $R_f$  and  $R_b$  are the internal reflection coefficients at the front and back surface of the cell,  $L$  is the total length of solar cell, and  $\phi_{ext}(\lambda)$  is the external incident photon flux. Eq. (6) and the parameters  $R_f$  and  $R_b$  describe the light trap of the solar cell.

### 3. Results and discussion

#### 3.1. Numerical model and parameters

As illustrated in Fig. 1, the structure of the crystalline silicon solar cell used in the simulation process is p–n–n<sup>+</sup>, where the TI impurity concentration in the n<sup>+</sup> layer is zero, and the corresponding thicknesses and the doping densities of the layers are (2  $\mu\text{m}$ ,  $N_A = 10^{18} \text{ cm}^{-3}$ ) (100  $\mu\text{m}$ ,  $N_D = 10^{17} \text{ cm}^{-3}$ ) and (20  $\mu\text{m}$ ,  $N_D = 10^{18} \text{ cm}^{-3}$ ), respectively. The parameters used in the simulation were given in Table 1. The model of Keevers and Green [3] and the model of Lucovsky [12] were used to calculate the electron and hole photoemission cross-sections of the impurity. In these two models  $\sigma_n^{opt}$  and  $\sigma_p^{opt}$  are assumed to be equal to zero for photons whose energy is greater than the band gap. The absorption of free carriers is not included into the model. The effects of TI concentration and the light trapping on the solar cell performance were investigated.

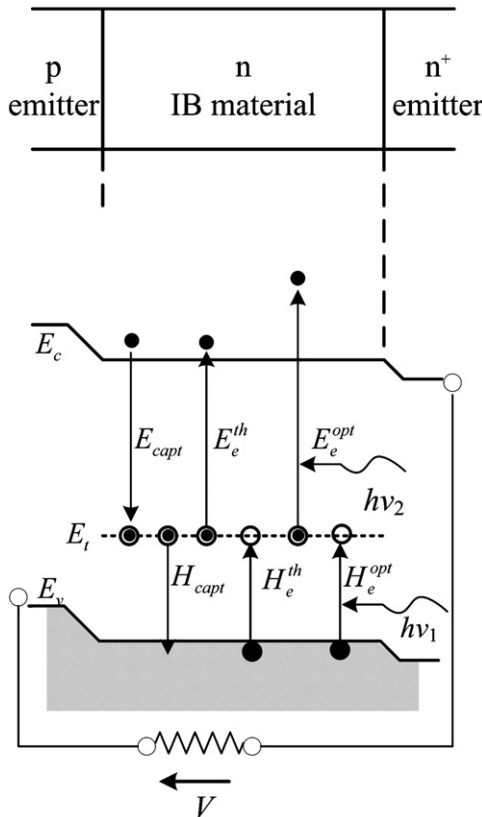


Fig. 1. Illustration of the fundamental operation of the IPV solar cell.

Table 1

Main parameters used in study (at 300 K) [3].

Property	Symbol	Value
Si energy gap (eV)	$E_g$	1.12
Electron mobility ( $\text{cm}^2/\text{V s}$ )	$\mu_n$	1350
Hole mobility ( $\text{cm}^2/\text{V s}$ )	$\mu_p$	480
Dielectric constant	$\epsilon_s$	11.7
Surface recombination velocity (cm/s)	$v_{sn}, v_{sp}$	10, $10^4$
TI energy level (eV)	$E_t - E_v$	0.26
Defect type		Acceptor
Electron thermal capture cross-section ( $\text{cm}^2$ )	$\sigma_n^{th}$	$1.0 \times 10^{-22}$
Hole thermal capture cross-section ( $\text{cm}^2$ )	$\sigma_p^{th}$	$5.07 \times 10^{-15}$

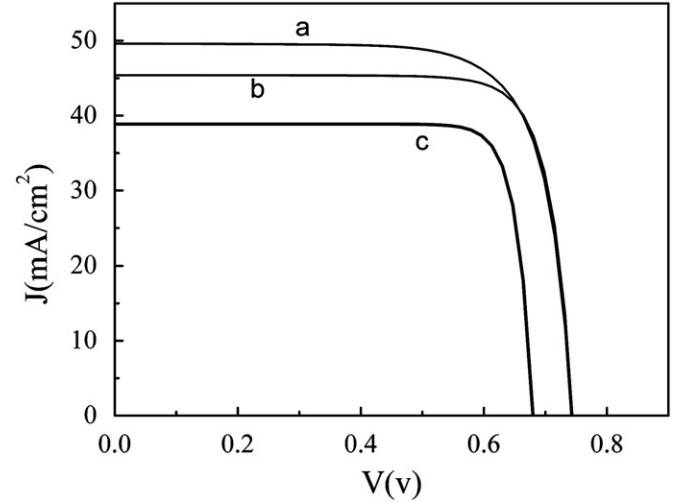
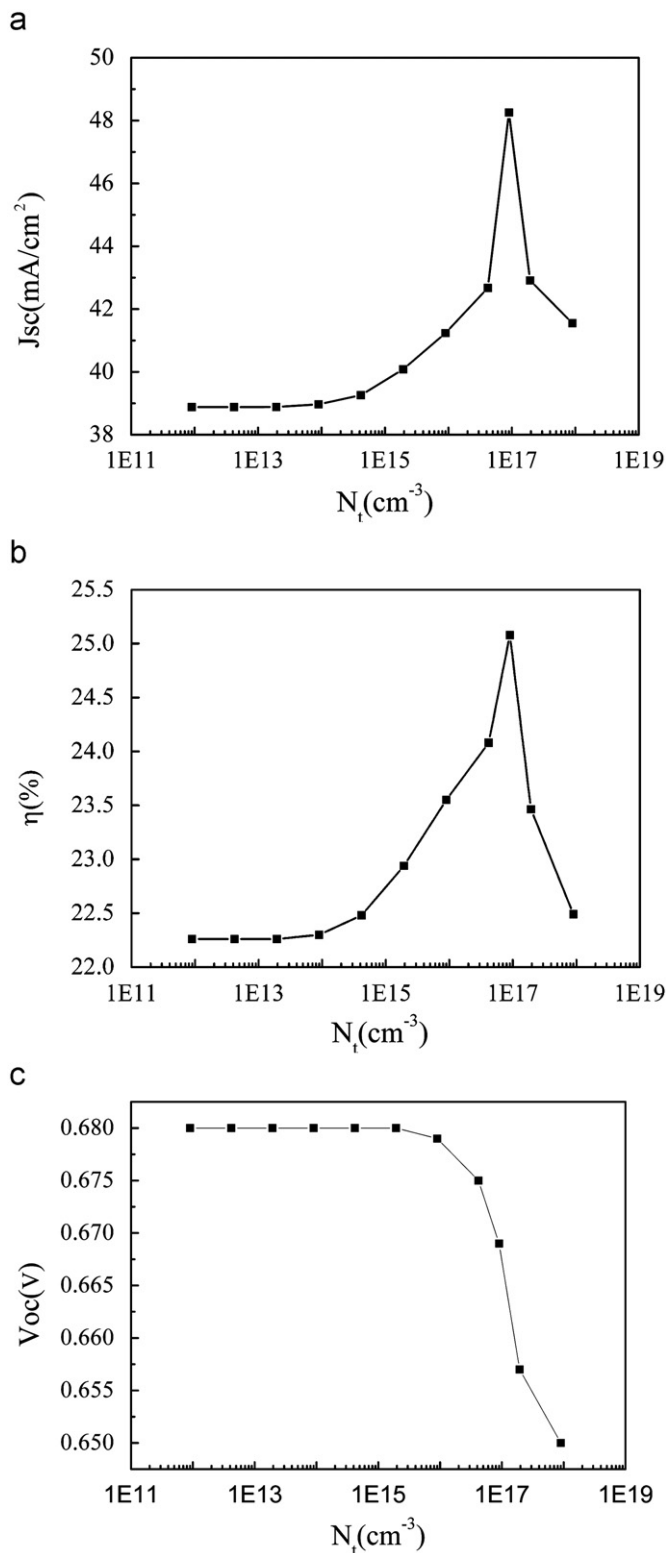


Fig. 2. Current–voltage characteristics for the p–n–n<sup>+</sup> silicon solar cell with  $R_b = R_f = 1$ . For curves a and b, the impurity concentration is  $N_t = 10^{17} \text{ cm}^{-3}$ . The optical generation via TI impurities is switched on for the curve a, but switched off for the curve b. For the curve c, TI concentration is set to zero.

The current–voltage characteristics for the p–n–n<sup>+</sup> silicon solar cell with an ideal light trapping ( $R_b = R_f = 1$ ) are shown in Fig. 2. The optical generation via TI impurities is switched on for the curve a. The optical generation via TI impurities is switched off for the curve b, but they can still contribute to the net doping and the recombination. The curve c corresponds to the case where there is no TI at all in the cell. It can be seen that the IPV effect clearly increases  $J_{sc}$  and  $\eta$ .

#### 3.2. The effect of thallium concentration

Fig. 3 shows the effect of TI impurity concentration  $N_t$  on the photovoltaic parameters: open-circuit voltage  $V_{oc}$ , photocurrent density  $J_{sc}$  and the conversion efficiency  $\eta$ . In Fig. 3, it can be seen that the highest efficiency was acquired at  $N_t = N_D = 10^{17} \text{ cm}^{-3}$ . The short-circuit current density and efficiency increase with increasing  $N_t$  only when  $N_t < N_D$ . But they decrease rapidly at impurity densities above the shallow base doping density ( $N_t > N_D$ ). The generation current due to TI impurity is governed by the slowest optical process, which is the transition, described by  $\sigma_n^{opt}$ , from TI level to CB [13]. If the impurity density is larger than the shallow doping density in the base ( $N_t > N_D$ ), the impurity defect level will not be fully occupied. As a result, the transition rate from the valence band to the impurity level is increased. The photon flux, available for the electron photoemission process from the defect to the conduction band, is reduced. Consequently the IPV effect is undermined.



**Fig. 3.** Solar cell parameters of an IPV Si solar cell as a function of the TI impurity concentration  $N_t$  calculated for  $N_D = 10^{17}$  cm<sup>-3</sup>. The internal reflections are set to  $R_f = 0.99$  and  $R_b = 0.99$ : (a) short-circuit current density  $J_{sc}$ , (b) conversion efficiency  $\eta$ , and (c) open-circuit voltage  $V_{oc}$ .

The open-circuit voltage decreases with increasing in impurity concentration. But it is still kept in moderate values before the impurity densities larger than the shallow doping density in the base ( $N_t > N_D$ ). This effect is due to the particular choice of the structure p–n–n<sup>+</sup>. This structure has an advantage to keep a high

value for the built-in voltage and thereafter keeps the TI level occupied. Therefore, the open-circuit voltage is safeguarded.

In practice, there are limits to the application of high TI concentrations to obtain a substantial IPV effect. Firstly, the density of the TI impurities is limited by the solid solubility of TI in Si. The method proposed by Olea et al. [14] may be able to break this limitation. Secondly, narrowing band gap will shift the intrinsic band-to-band absorption to lower energies, if  $N_D$  exceeds about  $10^{18}$  cm<sup>-3</sup>.

### 3.3. Effect of light trapping

Keever confirmed the importance of light trapping [3]. The ideal light trapping can maximize the optical path and increase optical absorption. They will increase solar cells' response to sub-band gap spectral. With ideal light trapping, a thinner base layer can be used to increase the collection of the minority carrier. In our model all effects of the optical management of the cell are incorporated in the values of the internal reflection  $R_f$  at the front and  $R_b$  at the back surface of the cell. We set the value  $R_f = 0.99$  and the degree of light trapping is adjusted by the value of  $R_b$ .  $R_b = 0$  stands for no light trapping, and  $R_b = 1$  stands for ideal light trapping.

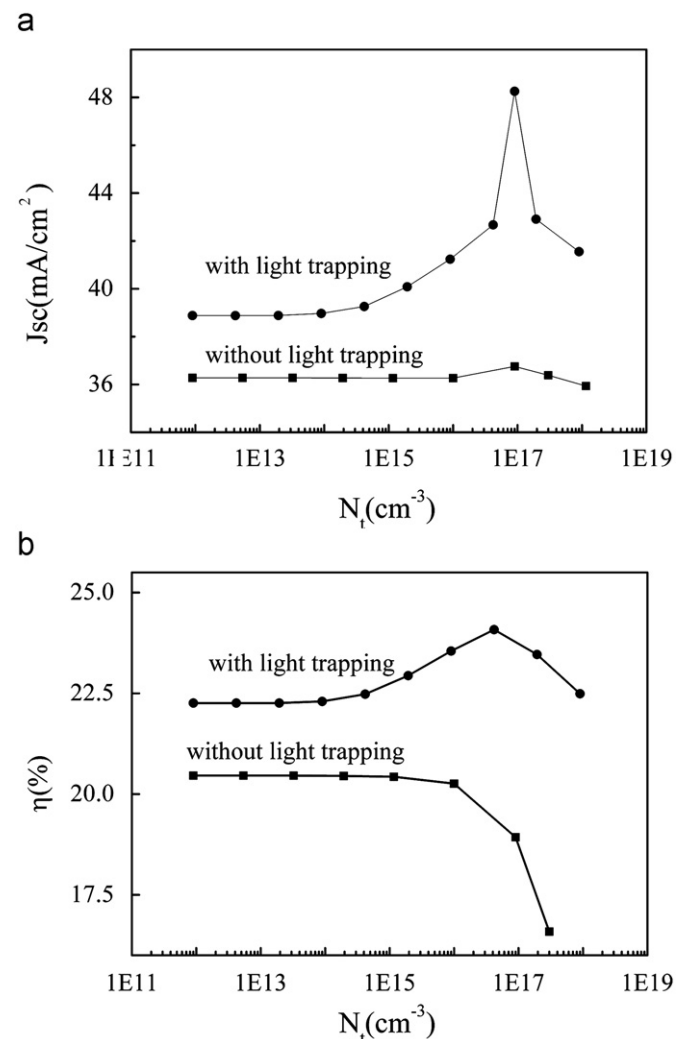


**Fig. 4.** Effect of light trapping on the IPV effect: (a) short-circuit current and (b) conversion efficiency.

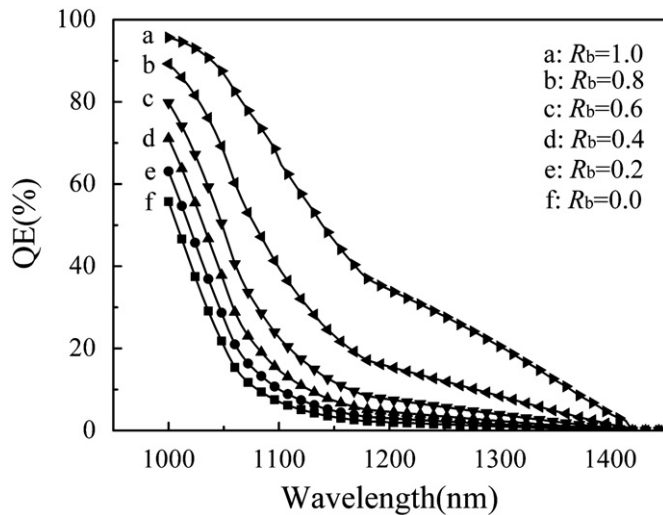


Fig. 5. Effect of light trapping on sub-bandgap spectral response with  $N_t = 10^{17} \text{ cm}^{-3}$ .

Fig. 4 shows the curves of  $J_{sc}(N_t)$  and  $\eta(N_t)$  with and without light trapping. The light trapping increases the short current by about  $9 \text{ mA/cm}^2$ , and the efficiency by about 2% (absolute) at the optimum Tl concentration  $N_t = 10^{17} \text{ cm}^{-3}$ . Without light trapping, the  $J_{sc}$  and the  $\eta$  are almost not improved. Because the IPV effect mainly increases the absorption of sub-band gap photons. Without light trapping, the penetration of long wave will undermine this enhancement.

Fig. 5 shows the spectral response curve of the IPV Si solar cells with different light trapping degree. It is further confirmed that the contribution of the IPV effect to the short-circuit current  $J_{sc}$  comes from sub-band gap absorption in the solar cell, which results in an extension of the infrared response, especially between 1000 and 1400 nm. The silicon solar cell doped with thallium has a better infrared response than that of doped with indium. For the IPV effect, there are two competing absorption mechanisms for the photons with energy between mid-gap and the full band gap. One photon is needed to excite an electron from the VB to the Tl level and another photon is needed to excite the electron from the Tl level to the CB. Only then can it contribute to the current. It is obviously reasoned that only half of those photons with energy between mid-gap and the full band gap will lead to an additional free electron–hole pair. Therefore, it seems better to have an impurity with energy level around one-third of

the band gap. The energy level of Tl is more suitable than that of In for crystalline Si solar cells.

#### 4. Conclusion

Using the numerical solar cell simulator SCAPS, the numerical study of the IPV effect in silicon solar cell doped with thallium as impurity was presented. The effects of Tl density and light trapping on the performance of Si solar cell were investigated. Results show that a significant improvement can be obtained in the short-circuit current and efficiency without too much sacrificing in open-circuit voltage. The effect of IPV increases with increasing the Tl concentration, until an optimum Tl concentration which equals around the base doping density. The IPV effect of thallium extends the spectral respond in the sub-band gap range from 1000 to about 1400 nm. A good light trapping structure is needed to observe significant IPV effect. With ideal light trapping ( $R_b = R_f = 0.99$ ), the IPV cell short current increases by about  $9 \text{ mA/cm}^2$ , and the efficiency by about 2%.

#### Acknowledgments

This work is supported by the Hunan Province Grand Science and Technology Special (Project no. 08FJ1002).

#### References

- [1] M. Schmeits, A.A. Mani, J. Appl. Phys. 85 (1999) 2207.
- [2] A. Luque, A. Mart, Phys. Rev. Lett. 78 (1997) 5014.
- [3] M.J. Keevers, M.A. Green, J. Appl. Phys. 75 (1994) 4022.
- [4] S. Khelifi, J. Verschraegen, M. Burgelman, A. Belghachi, Renew. Energy 33 (2008) 293.
- [5] S. Khelifi, M. Burgelman, J. Verschraegen, A. Belghachi, Sol. Energy Mater. Sol. Cells 92 (2008) 1559.
- [6] V.A. Morozova, O.G. Koshelev, E.P. Veretenkin, V.N. Gavrin, Y.P. Kozlova, Mosc. Univ., Moscow Univ. Phys. Bull. 64 (2009) 177.
- [7] S.Z. Karazhanov, J. Appl. Phys. 89 (2001) 4030.
- [8] A.S. Lin, W. Wang, J.D. Phillips, J. Appl. Phys. 105 (2009) 064512.
- [9] C.-T. Sah, P.C.H. Chan, C.-K. Wang, K.A. Yamakawa, R. Lutwack, R.L.-Y. Sah, IEEE Trans. Electron Devices 28 (1981) 304.
- [10] J. Verschraegen, S. Khelifi, M. Burgelman, A. Belghachi, in: Proceedings of the 21st European Photovoltaic Solar Energy Conference, Dresden, Germany 2006, p. 396.
- [11] M. Burgelman, P. Nollet, S. Degraeve, Thin Solid Films 361 (2000) 527.
- [12] G. Lucovsky, Solid State Commun. 3 (1965) 299.
- [13] J. Verschraegen, M. Burgelman, Thin Solid Films 515 (2007) 6276.
- [14] J. Olea, M. Toledano-Luque, D. Pastor, G. Gonzalez-Diaz, I. Martil, J. Appl. Phys. 104 (2008) 016105.